Published in final edited form as:
Exp Mol Pathol. 2013 February ; 94(1): 51–57. doi:10.1016/j.yexmp.2012.06.001.

Nef interaction with actin compromises human podocyte actin cytoskeletal integrity

Raymond Tan, **Hitesh Patni**, **Pranai Tandon**, **Liming Luan**, **Bipin Sharma**, **Divya Salhan**, **Moin A. Saleem**, **Peter W. Mathieson**, **Ashwani Malhotra**, **Mohammad Husain**, **Poornima Upadhya**, and **Pravin C. Singhal**
Department of Immunology, Feinstein Institute for Medical Research, North Shore LIJ Health System, New York, USA and Children's Renal Unit, University of Bristol, Bristol, United Kingdom

Abstract

The HIV-1 accessory protein Nef is considered to play an important role in the development of podocyte phenotype in HIV-1 associated nephropathy. We hypothesized that Nef may be altering podocyte phenotype both structurally and functionally. To elucidate the involved mechanisms, podocyte proteins interacting with Nef were identified using GST pull down assay and yeast two hybrid assay. The GST pull down assay on protein extracts made from stable colonies of conditionally immortalized human podocytes expressing Nef (Nef/CIHP) displayed a band at 45 kD, which was identified as actin by mass spectrometry. Yeast two hybrid assay identified the following Nef-interacting proteins: syntrophin, filamin B, syntaxin, translational elongation factor 1, and zyxin. The Nef-actin and Nef- zyxin interactions were confirmed by co-localization studies on Nef/CIHP stable cell lines. The co-localization studies also showed that Nef/CIHP stable cell lines had decreased number of actin filaments (stress fibers), displayed formation of lamellipodia, and increased number of podocyte projectons (filopodia). Nef/CIHP displayed enhanced cortical F-actin score index ($P<0.001$) and thus indicating reorganization of F-actin in the cortical regions. Microarray analysis showed that Nef enhanced the expression of Rac1, syndecan-4, Rif, and CDC42 and attenuated the expression of syndecan-3 and syntenin. In addition, Nef/CIHPs displayed diminished sphingomyelinase (ASMase) activity. Functionally, Nef/CIHPs displayed diminished attachment and enhanced detachment to their substrate. These findings indicate that Nef interaction with actin compromises podocyte cytoskeleton integrity.

Human immunodeficiency virus (HIV)-associated nephropathy (HIVAN) is a clinico-patholgical entity, which requires genetic (African ancestry, and genes such as APOL1), environmental (HIV-1 infection), and specific host factors for its manifestation (21). It is characterized by the collapsing variant of focal segmental glomerulosclerosis (FSGS) and microcystic dilatation of tubules (1, 31). Visceral epithelial cells (podocytes) have been demonstrated to play a key role in the pathogenesis of the collapsing variant of FSGS (4).

Podocytes are terminally differentiated and highly specialized cells with a complex cellular organization consisting of a cell body, major processes and foot processes (15, 18). The later form a characteristic interdigitating pattern with foot processes of adjacent podocytes,

Address for correspondence: Pravin C. Singhal, MD Division of Kidney Diseases and Hypertension 100 Community Drive Great Neck, NY11021 Tel 516-465-3010 Fax 516-465-3011 psinghal@nshs.edu.

forming in between the filtration slits which are bridged by the slit diaphragm, and thus serve as a filtration barrier. The foot processes contain an actin-based dynamic contractile apparatus, which also provide support to the capillary loops.

In HIV-1 transgenic mice, podocytes expressing HIV-1 genes develop renal lesions identical to HIVAN patients, which suggest the involvement of podocytes in HIVAN pathogenesis (32). In HIVAN, podocytes exhibit structural changes-loss of foot processes- which compromises the filtration barrier, both structurally and functionally (2). In addition, the HIVAN phenotype is characterized by collapse of capillary loops (11, 2, 21, 31).

HIV transgenic mouse studies have shown that HIV nephropathy is caused by renal expression of HIV gene products, and not because of indirect effects of HIV infection or altered cytokine milieu, thus, implicating a direct interaction between the HIV gene products and the host proteins in disease pathogenesis. HIV-1 encodes structural and accessory , two of the accessory proteins, Nef and Vpr (viral protein R) have been implicated as playing key roles in the pathology of HIVAN (2, 6, 23, 32). In animal studies, Nef has been shown to worsen the HIV nephropathy phenotype, although it may have a lesser role in disease induction (33). In-vitro cell studies have shown that Nef is responsible for podocyte proliferation and loss of podocyte differentiation markers (27).

Actin polymerizes into helical filaments in eukaryotic cells. These actin filaments further assembled into multiple higher order cellular structures, namely stress fibers, lamellipodia, filopodia, microvilli, each of which performs specific functions (10). Lamellipodia and filopodia are the protrusive structures at the leading edge of a cell, which are involved in cell migration or spreading. A lamellipodium is a thin (0.1-0.2 um) sheet-like protrusions that is filled with a branched network of actin and filopodia are thin finger like structures that are filled with tight parallel bundles of filamentous (F) actin. Nef has been shown to inhibit actin stress fiber formation and induced lamellipodia formation in podocytes (10). Earlier Klotman's group reported that Nef inhibited stress fiber formation but promoted lamellipodia formation in podocytes through the activation of Rac1 (16). Rac1 is a member of the Rac subfamily of the family Rho family of GTPases (5). Members of this superfamily appear to regulate a diverse array of cellular events, including the control of cell growth, cytoskeletal reorganization, and the activation of protein kinases. Under normal physiological conditions, Rac1 contributes to lamellipodia formation in differentiated cells (3).

In the present study, to further understand the role of Nef on podocyte injury associated with HIVAN, we identified the podocyte proteins that interact with Nef and evaluated the effect of Nef on the integrity of podocyte actin cytoskeleton. To determine the effect of Nef expression on podocyte adherent properties, we carried out attachment and detachment studies on Nef expressing podocytes.

Methods and Material

Preparation of human Podocytes

Human podocytes were obtained from Dr. Moin A. Saleem (Children's Renal Unit and Academic Renal Unit, University of Bristol, South Mead Hospital, Bristol, UK). Human podocytes were conditionally immortalized by introducing temperature-sensitive SV40-T antigen by transfection (24). The cells have additionally been transfected with a human telomerase construct (9). These cells proliferate at permissive temperature (33 °C, conditionally immortalized human podocytes) and enter growth arrest (CIHP) after transfer to the nonpermissive temperature (37 °C). The growth medium contains RPMI 1640 supplemented with 10% fetal bovine serum, 1× penicillin-streptomycin, 1 mML-glutamine,

and 1× insulin, transferrin, and selenium (ITS) (Invitrogen) to promote expression of T antigen.

Cloning of Nef gene in retroviral expression vectors and production of pseudotype retroviral supernatant

HIV-1 Nef gene was cloned in pBabe-puro retroviral expression vector (19) as described earlier at BamH I-Sal I restriction enzyme sites. Subsequently, Nef recombinant plasmid and empty vector were used to produce VSV G envelope pseudotyped viruses as described previously (14). In brief, Nef recombinant plasmid/empty vector was co-transfected in 293T cells along with the VSV.G envelope genes, which was provided *in trans* using pMD.G plasmid (gift of Dr. Didier Trono, Salk Institute, La Jolla, CA) (19), and the Moloney murine leukemia virus *gag/pol* genes using REP/GP plasmid to produce pseudotyped viruses.

Selection of Monoclonal Colonies

Human podocytes were transduced using above pseudotyped viruses containing Nef or empty vectors. The transduced podocytes were selected using growth medium containing Puromycin antibiotic (2.5 microgram/ml). Thereafter, human podocytes transduced with Nef or empty vector were subcultured and monoclonal colonies were isolated. The Nef expression was re-confirmed by western blotting.

Preparation of GST Nef protein

Bacteria (DH5α) were transformed with GST-NEF plasmid. Transformed bacteria were grown to an optical density of 0.45 before being induced with IPTG (0.75 mM). The culture medium was then centrifuged and resuspended in buffer A (0.5% NP-40, 20mM Tris at pH 8.0, 150 mM NaCl, 100 mM EDTA, protease inhibitor, PMSF). After sonication, the lysed bacterial culture was centrifuged and the supernatant was removed and mixed with glutathione sepharose beads (Amersham). The tube was centrifuged and the supernatant was discarded. The beads were washed twice with buffer A and then twice in buffer B (0.5% NP-40, 20 mM Tris at pH 8.0, 1 M NaCl, 1 mM EDTA, protease inhibitor, PMSF). 200 μL of elution (glutathione) buffer was added to the beads. The elution step was then repeated four times. The presence of GST-NEF protein was confirmed with Coomassie stain. A Sephadex G25 column was prepared with glass wool at the bottom of a 5 mL syringe. The eluent was passed through the column and centrifuged to remove glutathione. The centrifuged sample was stored at -80 degrees Celsius. The presence of GST-Nef was confirmed by Western blot (with probes for GST and Nef protein). A control sample of GST protein was prepared in the same manner as described above using pGEX. vector alone.

Preparation of radioactive cell lysate

Differentiated and undifferentiated human podocytes were grown to confluence on 150 mm culture dishes. Media deficient in methionine was prepared according to protocol. Keratinocyte media was used for HK-2 cells and RPMI was used for podocytes. 10% of heat-inactivated, dialyzed, fetal calf serum was added. Radioactive 35-S was added to deficient media at a concentration of 10 μCi per mL of media. Confluent cells were washed with PBS three times, then twice with deficient media (without radioactive 35-S). Radioactive, methionine deficient media was then added to the cells and incubated for three hours. Radioactive-labeled cell lysates were then prepared in the same method as described above.

GST-NEF and interacting protein binding

Cell lysates pre-cleared with glutathione sepharose beads were incubated with either 10 μg of GST or GST-NEF protein with glutathione sepharose beads for two hours at 4 degrees celsius on a gentle rocker. The mixtures were then centrifuged and the supernatants were discarded. The beads were washed three times with cold lysis buffer followed by two washes with 50 mM Tris at pH 8.0. The GST-glutathione sepharose beads were incubated in eluant (20 mM glutathione, 50 mM Tris at pH 8.0). The samples were then centrifuged and the supernatants were transferred to a fresh eppendorf tube. This process was repeated and the supernatants were combined for each sample.

Gel electrophoresis and Mass Spectroscopy

The samples obtained above were resolved in 10% SDS PAGE and the gel was stained with Coomassie blue. The GST-NEF protein and interacting radioactive-labeled samples were run on a separate gel. The gel with the radioactive samples was exposed for autoradiography. Protein bands on the Coomassie-stained gel that corresponded to bands on the autoradiogram were excised and sent for mass spectrometry at CTL Bioservices, Rockville, MD.

Yeast-Two Hybrid Screen

The Saccharomyces cerevisiae strain, AH109, yeast cells were transformed using a plasmid (pGBKT7) with either a cloned NEF or VPR gene. These plasmids were used to separately probe a pre-transformed AH109, complementary DNA library of human kidney tissue cloned into pGADT7 (Clontech, BD Biosciences). The yeast colonies with interacting proteins and activated GAL-4 transcription factor were selected using stringent criteria (SD media deficient in Leu, Trp, His, Ade). These colonies were then cultured and the pGADT7 plasmid was retrieved using a modified Mini-prep protocol (Qiagen). Yeast cells were resuspended in 67 mM potassium phosphate at pH 7.5, then lyticase was added and the mixture was heated to 37 degrees Celsius for two hours. The retrieved pGADT7 plasmids were used to transform DH5α cells. After selection on LB agar with ampicillin, positive growth colonies were extracted and plasmids were retrieved using Mini-prep protocol (Qiagen). These plasmids were then sequenced using primers (insert primer sequence) and the corresponding protein identity was obtained through the National Library of Medicine database.

Microarray analysis

Conditionally immortalized human podocytes (CIHP) were transduced with either HIV-1 Nef or EV, and stable colonies of Nef/CIHPs and EV/CIHPs were developed as described previously (10). Nef/CIHPs and EV/CIHPs were harvested and RNA was isolated, followed by microarray analysis. Microarray analysis was performed in duplicate samples with an Illumina Human V2-bead chip (Illumina, San Diego, CA) for 45,000 genes. In Nef/CIHPs, a total of 5,000 genes showed either upregulation or downregulation compared with vector-expressing podocytes.

Immunofluorescence studies

EV/CIHPs and Nef/CIHPs were plated on poly-D-lysine coated Lab-Tek culture slides. Cells were fixed and permeabilized with a buffer containing 0.02% Triton X-100 and 4% formaldehyde in PBS. Fixed cells were washed three times in PBS and blocked in 1% BSA for 30 min at 37°C. To detect Nef interaction with actin, cells were stained with rhodamine conjugated phalloidin (Molecular probe, to label actin) and FITC labeled anti-Nef antibody (AIDS Research reagent). Negative controls were performed in the presence of non-specific isotype antibody in place of primary antibody. Specific staining was visualized with an

inverted Olympus 1X 70 fluorescence microscopes equipped with a Cook Sensicom ER camera (Olympus America, Melville, NY.

Cortical F-actin score index (CFS)

EV/CIHPs and Nef/CIHPs grown on cover slips, were fixed with 4% paraformaldehyde for 10 min. The cells were permeabilized in 0.1% Triton X-100 for 10 min, blocked in 10% BSA in PBS for 1 h and incubated with phalloidin (Molecular Probes) washed and cells were incubated briefly in 4′-6-Diamidino-2-phenylindole (DAPI, Molecular Probes) for nuclei visualization. Images were obtained using an inverted fluorescent microscope. CFS index was determined based on three independent experiments. In each experiment, 10 images were taken blindly from each group. All imaged cells were counted using DAPI stained nuclei and assessed as follows. The F-actin cytoskeletal reorganization for each cell was scored on a scale ranging from 0 to 3 based on the degree of cortical F-actin ring formation (score=0, no cortical F-actin, normal stress fibers; score=1, cortical F-actin deposits below ½ the cell border; score=2, cortical F-actin deposits exceeding 1/2 the cell border; score=3, complete cortical ring formatting and/or total absence of central stress fiber. A minimum of 100 cells were examined in the 10 images from every group in each independent experiment, and the CFS index for normal and treated podocytes is the ratio of average score of the counted cells to cell counted (22).

ASMase activity

ASMase activity was measured in EV/CIHPs and Nef/CIHPs. The lysates were collected in acetate buffer (50 mM, pH 5.0) and subjected to freeze/thaw (–80°C) without the addition of protease or phosphatase inhibitors. ASMase activity was measured with a two-step procedure using the Amplex Red Sphingomyelinase kit (Molecular Probes/Invitrogen Corp.) and was normalized for protein content. Fluorescence was measured with a fluorescence microplate reader using excitation/emission wavelengths of 530/590 nm.

Statistical analysis

For comparison of mean values between two groups, the unpaired t test was used. To compare values between multiple groups, analysis of variance (ANOVA) was applied and a Bonferroni multiple range test was used to calculate a p-value. Statistical significance was defined as $P<0.05$. All values are displayed as mean ± SD.

Results

Identification of Nef-interacting proteins in renal epithelial cells

Two distinct protein bands with approximate molecular weights of 132 kD and 45 kD were seen in all three cell lines (tubular cells, undifferentiated podocytes, and differentiated podocytes). These protein bands appeared only in the GST-Nef lanes and not in the control lanes (Fig 1). Mass spectrometry further identified these proteins to be most likely myosin 1C (132 kD) and actin (45 kD).

Cloning of Nef-interacting proteins by using yeast two hybrid system

Nef-interacting proteins were cloned using yeast two hybrid system. Over 100 different colonies of yeast with NEF-interacting proteins were sequenced. Of those listed, most are involved in the cytoskeleton or in cell signaling. NEF-interacting proteins of interest are shown in Table 1.

Nef/CIHPs display altered actin cytoskeleton and phenotype

To determine alteration in phenotype, EV/CIHPs and Nef/CIHPs were examined under light microscope. Representative microphotographs of EV/CIHP and Nef/CIHPs are shown in Fig. 2 as inset. Nef/CIHP displayed altered morphology when compared to EV/CIHPs. Nef/CIHPs appeared less spread and were not elongated, whereas, EV/CIHP were well spread and elongated (Fig. 2). Total of 200 cells were counted in four sets of experiments. Cumulative data are shown in a bar diagram.

To determine the effect of Nef on actin cytoskeleton, EV/CIHP and Nef/CIHPs were labeled with phalloidin and DAPI (nuclear stain). Nef/CIHP displayed scanty actin filament and presence of cortical F-actin (Fig. 3). Total of 100 cells were examined. Cumulative data of four sets of experiments are shown in bar graphs. Cortical F-actin score was higher ($P<0.001$) in Nef/CIHPs when compared to EV/CIHPs.

Nef colocalizes with cortical F-actin in Nef/CIHPs

Since Nef interacted with actin in yeast two hybrid system, we carried out double labeling studies for Nef and actin in Nef/CIHPs and EV/CIHPs. Nef/CIHPs and EV/CIHPs were labeled with phalloidin (for visualization of actin fibers) and with anti-Nef antibody (for colocalization). Representative microphotographs are shown in Fig. 4. EV/CIHPs displayed brightly fluorescent actin filaments. On the other hand, Nef/CIHPs showed cortical F-actin and at place it colocalized with Nef (indicated by orange color). The actin cytoskeleton was reorganized to form more lamellipodia (deposition of actin at cortical regions) as well as filopodia (projections) in Nef /CIHPs. Both formation of lamellipodia and filopodia were scanty in EV/CIHPs (Fig. 4). Cumulative data from four sets of experiments displaying percentage of EV/CHP and Nef/CHP manifesting filopodia are shown in Fig. 4.

Nef/CIHPs display co-localization of Nef with zyxin

Since zyxin is considered an actin filament repair protein, we expected higher expression of zyxin in Nef/CIHPs. To determine zyxin expression, EV/CIHPs and Nef/CIHPs were immunolabeled for Nef and zyxin. Representative microphotographs of EV/CIHPs and Nef/CIHPs are shown in Fig. 5. Nef/CIHPs displayed peripheral distribution of Zyxin as compared to diffuse distribution in Ev/CIHP

Nef/CIHPs showed enhanced expression of Rac1 and CDC42

RAC activity promotes the protrusion of the lamellipodium and CDC42 controls the formation and propagation of filopodium (3, 5, 16). We hypothesized that Nef may enhancing podocyte display of lamellipodia and filopodia by enhancing transcription of Rac1 and CDC42 respectively. To determine mRNA expression, total RNAs were extracted from Nef/CIHPs and EV/CIHPs (n=2). Microarray analysis was performed in duplicate samples with an Illumina Human V2-bead chip for 45,000 genes. In Nef/CIHPs, a total of 5,000 genes showed either upregulation or downregulation compared with vector-expressing podocytes. Nef/CIHPs showed several fold upregulation of RAC, Rif, and CDC42, as compared to EV/CIHPs (Table 2). RAC and CDC42 expression was found to be 11.9 and 2.7 times higher respectively, in Nef/CIHPs when compared to EV/CIHPs (Fig. 6).

Nef/CIHPs display attenuated ASMase activity

In a recent report, decreased ASMase activity in podocytes was shown to be associated with altered actin cytoskeleton (11). To determine, whether Nef may be altering podocyte actin cytoskeleton by attenuating ASMase activity, cellular lysates of EV/CIHPs and Nef/CIHPs were assayed for ASMase activity. EV/CIHPs displayed attenuated ASMase activity (Fig.

7). These findings indicate that Nef-induced attenuated ASMase activity may also be contributing to altered actin cytoskeleton in Nef/CIHPs.

Nef decreases podocyte adherence

To determine adherence of NEF/CIHPs to the substrate, we carried out detachment assay on Nef/CIHPs and EV/CIHPs. Majority of Nef/CIHPs (95%) and only 45% of EV/CIHPs were detached after 5 minutes of trypsinization (0.05% trypsin) (Fig. 8). Results of experiments performed with 0.025% trypsin were similar and were statistically significant (Data not shown).

To determine the time course effect of attachment of Nef/CIHPs, equal number of Nef/CIHPs and EV/CIHPs were plated into 24 hour well plates, and the number of unattached cells in the media, were counted at different time intervals. At 2 hour interval, only 8% of EV/CIHPs were unattached to the culture plate when compared to 20% of Nef/CIHPs (Fig. 9).

Discussion

In the present study, we demonstrated the interaction of Nef with actin by using GST pull down assay. Nef and actin interaction led to the loss of stress fibers in Nef/CIHPs. In addition, Nef/CIHPs displayed enhanced formation of lamellipodia. Interestingly, Nef increased F-actin content in podocytes (Data not shown). Since actin cytoskeleton of podocytes in general and foot processes in particular provide support to the maintenance of capillary loop phenotype, compromised cytoskeletal integrity of foot processes' due to Nef – actin interaction might have contributed to capillary collapse in HIVAN. In addition, Nef-induced decreased adherence to the substrate make podocytes vulnerable to detach from the glomerular basement membrane. Micro-array analysis revealed enhanced expression of Rac1, Rif, and CDC42 by Nef/CIHPs. It appears that Nef-induced Rac1 expression may be contributing to increased number of lamellipodia in Nef/CIHPs. Nef-induced formation of lamellipodia and filopodia might have enhanced podocyte motility into the Bowman's space. Nef/CIHPs also displayed attenuated ASMase activity, which might have contributed to altered actin cytoskeleton.

Actin-disrupting role of Nef has been considered to play a critical role in HIV-1 replication (23). Nef promotes the loss of stress fibers and enhances the formation of lamellipodia in podocytes (16). These effects of Nef are attributed to the activation of Rac1 and RhoA inhibition. Several investigators identified an interaction between Nef and diaphanous interacting protein (DIP), a regulator of Rho and Rac signaling (5, 16). These investigators demonstrated that in HIV-infected podocytes, Nef, through the recruitment of DIP and p190 RhoAGAP to Nef-Src complex, activated p190RhoAGAP and down-regulatedRhoA activity. Other investigators also studied the role of Rac1 in actin organization in mouse podocytes (10). In differentiated podocytes, Rac1 activity increased significantly and was associated with more lamellipodia formation (3). Similarly, transient transfection of constitutively active Rac1 markedly increased the number of lamellipodia in undifferentiated mouse podocytes; on the other hand, the Rac1 inhibitor caused actin cytoskeleton derangement in differentiating mouse podocytes (3). Rac1 has also been demonstrated to stimulate actin filament accumulation at the plasma membrane, forming membrane ruffles in other cells such as fibroblasts (22). In the present study, Nef expressing human podocytes not only showed enhanced expression of Rac1, but also demonstrated loss of stress fibers and increased number of lamellipodia. These findings in human podocytes are consistent with other investigators who studied the effect of Nef on mouse podocytes.

The formation of lamellipodia is thought to be regulated almost entirely by the assembly of an intricate network of F-actin and actin-associated proteins. It is well established that actin filaments, the Arp 2/3 complex and N-WASP (2, 25), regulated by various small Rho-family GTPases (e.g., Rac1) and actin capping/binding proteins (cofilin and profilin) are universal components of lamellipodia. CDC42 modulates Filopodia formation. Expression of RAC1 and CDC42 were found to be up regulated in Nef/CIHPs. CDC42 activity was unchanged in prior reports (10), however, increased efficiency of Nef secondary to selection of monoclonal colonies might have contributed to this difference.

To maintain the structural integrity of actin cyoskeleton, cells have to recognize and respond to stress posed to the actin filaments (stress fibers) at the leading edge during their spread. Zyxin has been demonstrated to play a key role in the maintenance of the integrity of stress fibers in the presence of ongoing stress (26). Normally, stress transmission capabilities of actin filaments are compromised after force-induced elongation and thinning events; nonetheless, these events are followed by actin filaments fiber repair, which restores their stress transmission capabilities (20, 26). Zyxin rapidly accumulates at the sites of damage of stress fibers and is essential for the repair of actin filaments and generation of traction force (26). Another protein, a-actinin (an actin regulatory protein) also plays an essential role in restoration of actin integrity at sites of actin filament damage. Besides α-actinin, VASP also limits elongation of the stress fibers at strain sites, and thus promotes stabilization of the stress fiber (26). Interestingly, zyxin promotes recruitment of both α-actinin and VASP to the zones of compromised stress fiber. In the present study, Nef/CIHPs displayed co-localization of zyxin at the periphery of cells. Since Nef/CIHPs showed only scant number of actin filaments it appears that accumulation of zyxin was an exercise in futile to repair the stress fibers. Alternatively, enhanced expression of zyxin provided a rather limited stability to Nef/CIHPs by repairing only a few partially injured stress fibers. The later provided the maintenance of cellular phenotype despite the loss of cytoskeletal integrity–loss of significant number of stress fibers- in Nef/CIHPs.

Podocytes adhere to the glomerular basement membrane by cell surface receptors which bind to heparan sulfate glycosaminoglycan chains (8). Reduction in heparan sulfate associated anionic sites in the glomerular basement membrane of rats with streptozotocin-induced diabetic nephropathy was associated with proteinuria (29). It is possible that lack of adhesion molecules such as heparan sulfate might have contributed to the loss of podocytes and thus manifesting as podocytopenia in diabetic nephropathy. In the present study, Nef/CIHPs showed diminished expression of proteoglycan syndecan-3. Role of Syndecan 3 in the organization of cell shape by affecting the actin cytoskeleton has been suggested previously (30). It is possible that Nef might be inducing podocyte injury through decreased podocyte expression of syndecan-3 and associated loss of adhesion of podocytes to glomerular basement membrane in Nef transgenic mice. In the present study, Nef/CIHPs displayed diminished adherence.

In an *in vitro* study, the investigators evaluated adhesion properties of control and mutant (without heparan sulfate glycosaminglycan chain) cultured mouse podocytes (30). In adhesion assays, control podocytes attached, spread, and migrated more efficiently than to mutant podocytes. Syndecan-4 was localized to focal adhesions in control podocytes coinciding with stress fiber formation; whereas, in mutant cells, syndecan-4 was associated with smaller focal contacts and cortical actin organization (30). Further analysis by flow cytometry displayed that mutant cells had twice the amount of surface syndecan-4 to that of normal cells. These studies suggested formation of focal points, cortical organization, and adhesion was compromised because of the lack of ligand-receptor interaction in mutant podocytes. In the present study, Nef/CIHP displayed increased expression of syndecan-4. Since Nef/CIHPs not only showed robust expression of Rac1 but also showed its effects in

the form of scant stress fibers and enhanced lamellipodia, it appeared that enhanced expression of syndecan-4 by Nef/CIHP might be occurring as a compensatory response.

The small GTPase Rif and its effector mDia2 formin have been reported to play play a central role in regulating actin dynamics during filopodia elongation (12). Nef/CIHPs displayed RIF mRNA expression 4.5 fold higher when compared to EV/CIHPs. It will be important to study the role of this molecule in future studies.

In a recent report, down regulation of sphingomyelinase (ASMase) activity was associated with loss of actin filaments in podocytes (11). On the other hand, rituximab partially prevented ASMase down-regulation and restored podocyte phenotype. The author suggested the role of ASMase activity in the development of recurrence of focal glomerulosclerosis in kidney transplant patients. In the present study, Nef/CIHPs also displayed diminished ASMase activity. It is likely that Nef induced diminished ASMase activity might have also contributed to altered podocyte actin cytoskeleton. It will be interesting to further investigate the role of ASMase in the Nef induced altered actin cytoskeleton in future studies.

We conclude that the interaction of Nef with actin compromises cytoskeletal integrity of human podocytes and may be responsible for the loss of adhesion properties of the podocytes. The present study provides an insight into the Nef-induced podocyte injury in patients with HIVAN and also provides therapeutic targets for drug intervention.

Acknowledgments

This work was supported by grants RO1DK084910 and RO1 DK083931 (PCS) from National Institutes of Health, Bethesda, MD. We are thankful to AIDS Reagent Program for providing anti-Nef antibody.

References

1. Atta MG. Diagnosis and natural history of HIV-associated nephropathy. Adv Chronic Kidney Dis. 2010; 17:52–8. [PubMed: 20005489]
2. Atta MG, Lucas GM, Fine DM. HIV-associated nephropathy: epidemiology, pathogenesis, diagnosis and management. Expert Rev Anti Infect Ther. 2008; 6:365–71. [PubMed: 18588500]
3. Attias O, Jiang R, Aoudjit L, Kawachi H, Takano T. Rac1 contributes to actin organization in glomerular podocytes. Nephron Exp Nephrol. 2010; 114:e93–e106. [PubMed: 19955829]
4. Barisoni L, Mokrzycki M, Sablay L, Nagata M, Yamase H, Mundel P. Podocyte cell cycle regulation and proliferation in collapsing glomerulopathies. Kidney Int. 2000; 58:137–43. [PubMed: 10886558]
5. Bosco EE, Mulloy JC, Zheng Y. Rac1 GTPase: a “Rac” of all trades. Cell Mol Life Sci. 2009; 66:370–4. [PubMed: 19151919]
6. Bruggeman LA, Dikman S, Meng C, Quaggin SE, Coffman TM, Klotman PE. Nephropathy in human immunodeficiency virus-1 transgenic mice is due to renal transgene expression. J Clin Invest. 1997; 100:84–92. [PubMed: 9202060]
7. Campbell EM, Nunez R, Hope TJ. Disruption of the actin cytoskeleton can complement the ability of Nef to enhance human immunodeficiency virus type 1 infectivity. J Virol. 2004; 78:5745–55. [PubMed: 15140972]
8. Chen S, Wassenhove-McCarthy D, Yamaguchi Y, Holzman L, van Kuppevelt TH, Orr AW, Funk S, Woods A, McCarthy K. Podocytes require the engagement of cell surface heparan sulfate proteoglycans for adhesion to extracellular matrices. Kidney Int. 2010; 78:1088–99. [PubMed: 20463653]
9. Coward RJ, Welsh GI, Koziell A, Hussain S, Lennon R, Ni L, Tavaré JM, Mathieson PW, Saleem MA. Nephrin is critical for the action of insulin on human glomerular podocytes. Diabetes. 2007; 56:1127–1135. [PubMed: 17395751]

10. Defilippi P, Olivo C, Venturino M, Dolce L, Silengo L, Tarone G. Actin cytoskeleton organization in response to integrin-mediated adhesion. Microsc Res Tech. 1999; 47:67–78. [PubMed: 10506763]
11. Fornoni A, Sageshima J, Wei C, Merscher-Gomez S, Aguillon-Prada R, Jauregui AN, Li J, Mattiazzi A, Ciancio G, Chen L, Zilleruelo G, Abitbol C, Chandar J, Seeherunvong W, Ricordi C, Ikehata M, Rastaldi MP, Reiser J, Burke GW 3rd. Rituximab targets podocytes in recurrent focal segmental glomerulosclerosis. Sci Transl Med. 2011; 3:85ra46.
12. Hotulainen P, Llano O, Smirnov S, Tanhuanpää K, Faix J, Rivera C, Lappalainen P. Defining mechanisms of actin polymerization and depolymerization during dendritic spine morphogenesis. J Cell Biol. 2009; 185:323–39. [PubMed: 19380880]
13. Hsu HH, Hoffmann S, Endlich N, Velic A, Schwab A, Weide T, Schlatter E, Pavenstädt H. Mechanisms of angiotensin II signaling on cytoskeleton of podocytes. F actin scoring. J Mol Med. 2008; 86:1379–139. [PubMed: 18773185]
14. Husain M, Gusella GL, Klotman ME, Gelman IH, Ross MD, Schwartz EJ, Cara A, Klotman PE. HIV-1 Nef induces proliferation and anchorage-independent growth in podocytes. J Am Soc Nephrol. 2002; 13:1806–15. [PubMed: 12089376]
15. Kriz W, Elger M, Mundel P, Lemley KV. Structure-stabilizing forces in the glomerular tuft. Am Soc Nephrol. 1995; 5:1731–9.
16. Lu TC, He JC, Wang ZH, Feng X, Fukumi-Tominaga T, Chen N, Xu J, Iyengar R, Klotman PE. HIV-1 Nef disrupts the podocyte actin cytoskeleton by interacting with diaphanous interacting protein. J Biol Chem. 2008; 283:8173–82. [PubMed: 18234668]
17. Morgenstern JP, Land H. Advanced mammalian gene transfer: High titre retroviral vectors with multiple drug selection markers and a complementary helper-free packaging cell line. Nucleic Acids Res. 1990; 18:3587–3596. [PubMed: 2194165]
18. Mundel P, Kriz W. Structure and function of podocytes: an update. Anat Embryol. 1995; 19:385–97. [PubMed: 8546330]
19. Naldini L, Blomer U, Gallay P, Ory D, Mulligan R, Gage FH, Verma IM, Trono D. In vivo gene delivery and stable transduction of non-dividing cells by a lentiviral vector. Science. 1996; 272:263–267. [PubMed: 8602510]
20. Nguyen TN, Uemura A, Shih W, Yamada S. Zyxin-mediated actin assembly is required for efficient wound closure. J Biol Chem. 2010; 285:35439–45. [PubMed: 20801875]
21. Papeta N, Sterken R, Kiryluk K, Kalyesubula R, Gharavi AG. The molecular pathogenesis of HIV-1 associated nephropathy: recent advances. Mol Med. Jan 11.2011
22. Ridley AJ, Paterson HF, Johnston CL, Diekmann D, Hall A. The small GTP-binding protein rac regulates growth factor-induced membrane ruffling. Cell. 1992; 70:401–10. [PubMed: 1643658]
23. Rosenstiel P, Gharavi A, D'Agati V, Klotman P. Transgenic and infectious animal models of HIV-associated nephropathy. J Am Soc Nephrol. 2009; 20:2296–304. [PubMed: 19497967]
24. Saleem MA, O'Hare MJ, Reiser J, Coward RJ, Inward CD, Farren T, Xing CY, Ni L, Mathieson PW, Mundel P. A conditionally immortalized human podocyte cell line demonstrating nephrin and podocin expression. J. Am. Soc. Nephrol. 2002; 13:630–638. [PubMed: 11856766]
25. Small JV, Stradal T, Vignal E, Rottner K. The lamellipodium: where motility begins. Trends Cell Biol. 2002; 12:112–120. [PubMed: 11859023]
26. Smith MA, Blankman E, Gardel ML, Luettjohann L, Waterman CM, Beckerle MC. A zyxin-mediated mechanism for actin stress fiber maintenance and repair. Dev Cell. 2010; 19:365–76. [PubMed: 20833360]
27. Sunamoto M, Husain M, He JC, Schwartz EJ, Klotman PE. Critical role for Nef in HIV-1-induced podocyte dedifferentiation. Kidney Int. 2003; 64:1695–701. [PubMed: 14531802]
28. Takenawa T, Suetsugu S. The WASP-WAVE protein network: connecting the membrane to the cytoskeleton. Nat Rev Mol Cell Biol. 2007; 8:37–48. [PubMed: 17183359]
29. van den Born J, van Kraats AA, Bakker MA, Assmann KJ, Dijkman HB, van der Laak JA, Berden JH. Reduction of heparan sulphate-associated anionic sites in the glomerular basement membrane of rats with streptozotocin-induced diabetic nephropathy. Diabetologia. 1995; 38:1169–75. [PubMed: 8690168]

30. Woods A. Syndecans: transmembrane modulators of adhesion and matrix assembly. J Clin Invest. 2001; 107:935–941. [PubMed: 11306594]

31. Yadav A, Vallabu S, Kumar D, Ding G, Charney DN, Chander PN, Singhal PC. HIVAN phenotype: consequence of epithelial mesenchymal transdifferentiation. Am J Physiol Renal Physiol. 2010; 298:F734–44. [PubMed: 20015943]

32. Zhong J, Zuo Y, Ma J, Fogo AB, Jolicoeur P, Ichikawa I, Matsusaka T. Expression of HIV-1 genes in podocytes alone can lead to the full spectrum of HIV-1-associated nephropathy. Kidney Int. 2005; 68:1048–60. [PubMed: 16105035]

33. Zuo Y, Matsusaka T, Zhong J, Ma J, Ma LJ, Hanna Z, Jolicoeur P, Fogo AB, Ichikawa I. HIV-1 genes vpr and nef synergistically damage podocytes, leading to glomerulosclerosis. J Am Soc Nephrol. 2006; 17:2832–43. [PubMed: 16988066]

Highlights (for review)

- Podocyte have been demonsrated to have unique phenotype in HIV-associated nephropathy.
- Podocyte proteins interacting with Nef were identified using GST pull down assay and yeast two hybrid assay.
- Yeast two hybrid assay identified the following Nef-interacting proteins: syntrophin, filamin B, syntaxin, translational elongation factor 1, and zyxin.
- The co-localization studies also showed that Nef/CIHP stable cell lines had decreased number of actin filaments (stress fibers), displayed formation of lamellipodia, and increased number of podocyte projectons (filopodia).
- Microarray analysis showed that Nef enhanced the expression of Rac1, syndecan-4, Rif, and CDC42 and attenuated the expression of syndecan-3 and syntenin.
- The altered phenotype seemed to be the outcome of the interaction between Nef and actin.

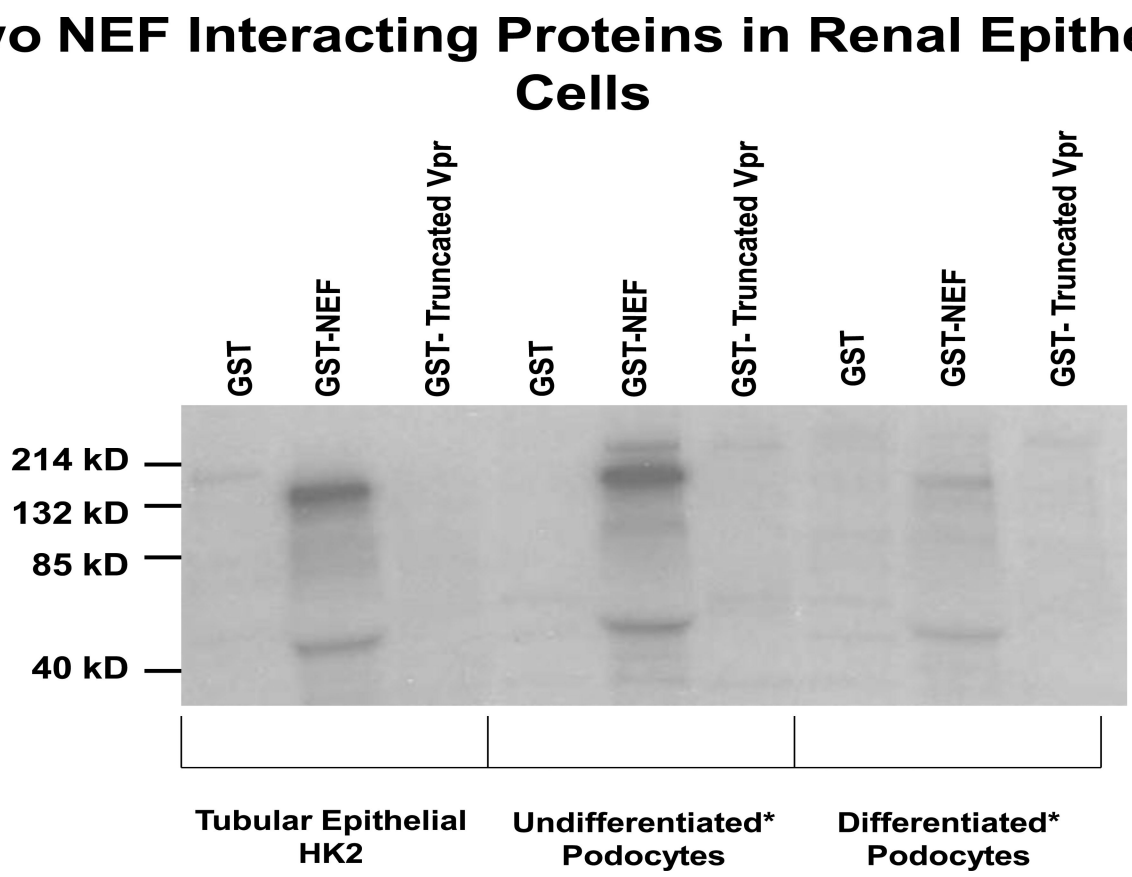

1. Renal epithelial cells display Nef-interacting proteins

GST and GST fusion protein coupled to glutathione Sepharose beads were incubated for 2 h at 4 °C with end-over-end mixing with cell lysates from 35S-labeled cells of human proximal tubular epithelial cells (HK2), undifferentiated CIHPs and differentiated CIHPs. The cell lysates were pre cleared with GSH buffer and GST to prevent interaction with proteins which binds to GST alone. The beads were washed four times with PBS, and the bound radioactive proteins were subjected to SDS-PAGE and visualized by a phosphor imager. Representative gels from HK2s, undifferentiated and differentiated podocytes are shown.

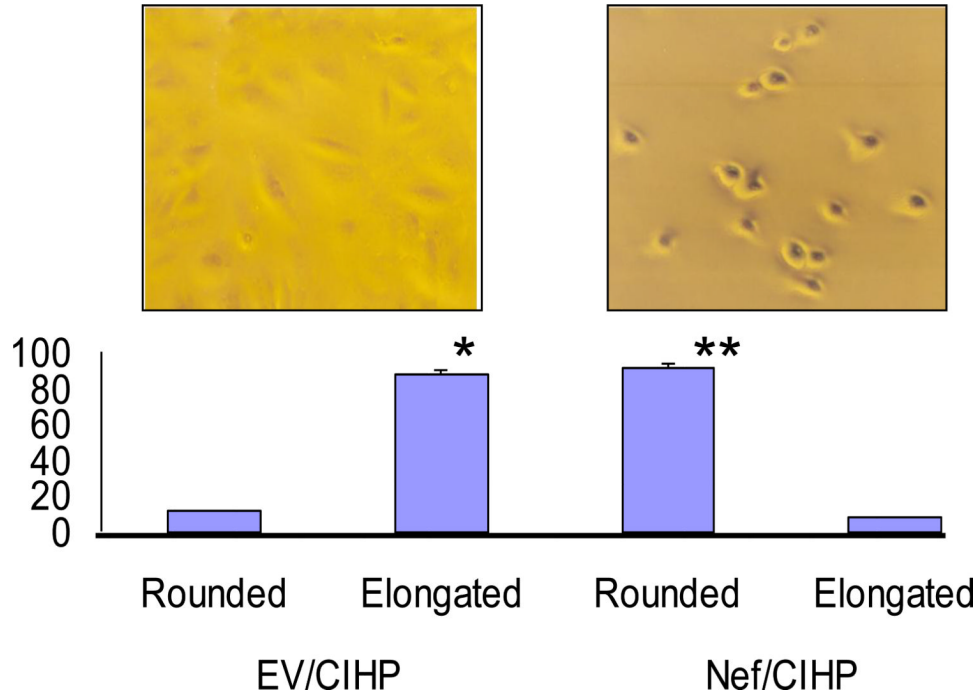

2. Nef/CIHPs display altered phenotype

EV/CIHPs and Nef/CIHPs grown on Petri dishes were examined under light microscope. Representative microphotographs of EV/CIHP and Nef/CIHPs are shown as inst. Nef/CIHP displayed altered morphology when compared to EV/CIHPs. Total of 200 cells were counted in four sets of experiments. Cumulative data are shown in a bar diagram.

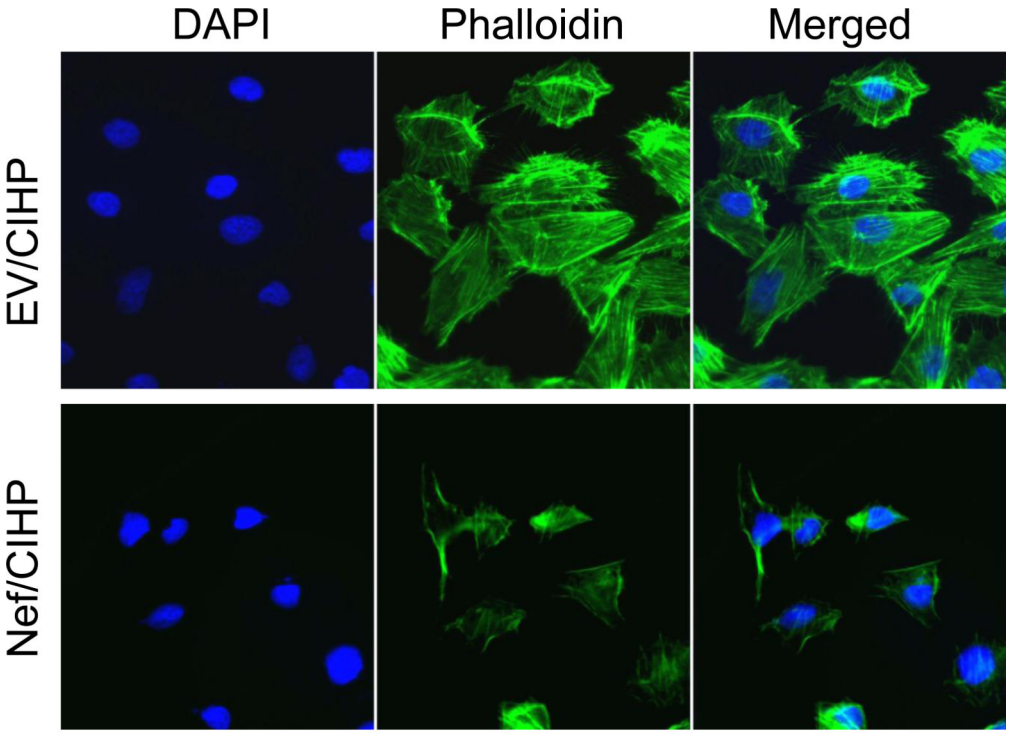

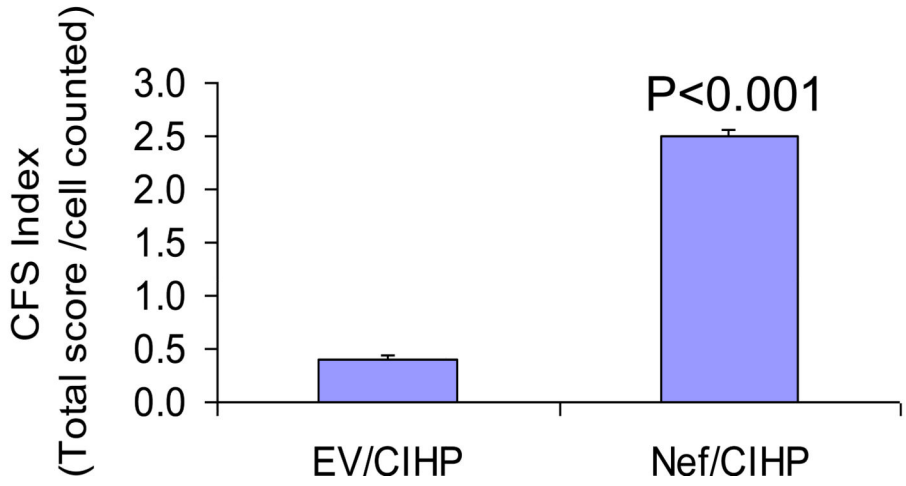

3. Nef/CIHPs display altered actin cytoskeleton

EV/CIHP and Nef/CIHPs were labeled with phalloidin and DAPI (nuclear stain). Nef/CIHP displayed scanty actin filament and presence of cortical F-actin. Total of 100 cells were examined. Cumulative data of four sets of experiments are shown in bar graphs.

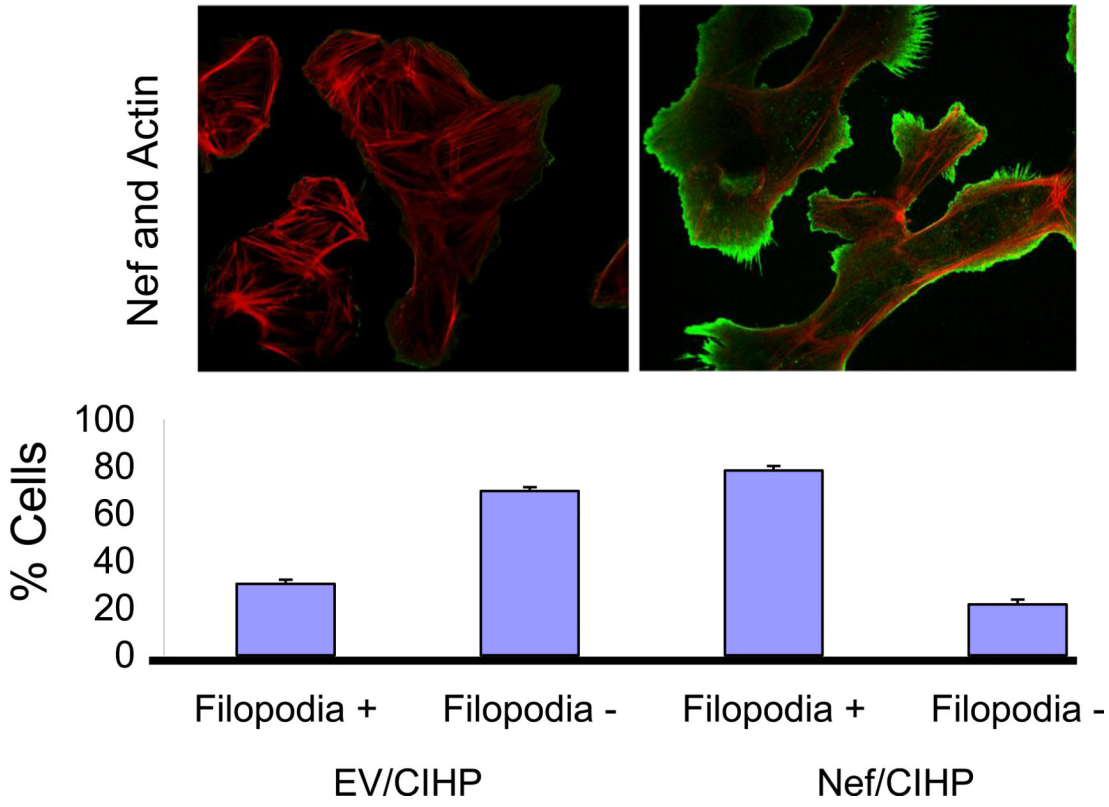

4. Nef/CIHPs display scant actin filaments and enhanced formation of lamellipodia and filopodia

Nef/CIHPs and EV/CIHPs were immunolabeled with phalloidin and anti-Nef antibody. Representative microphotographs are shown. EV/CIHPs displayed brightly fluorescent actin filaments; whereas, Nef/CIHPs showed a few actin filaments and orange color in cortical regions indicating co-localization with Nef. Nef/CIHPs dispayed both lamellipodia and filopodia. Cumulative data on percentage of cells showing filopodia are show in bar graphs.

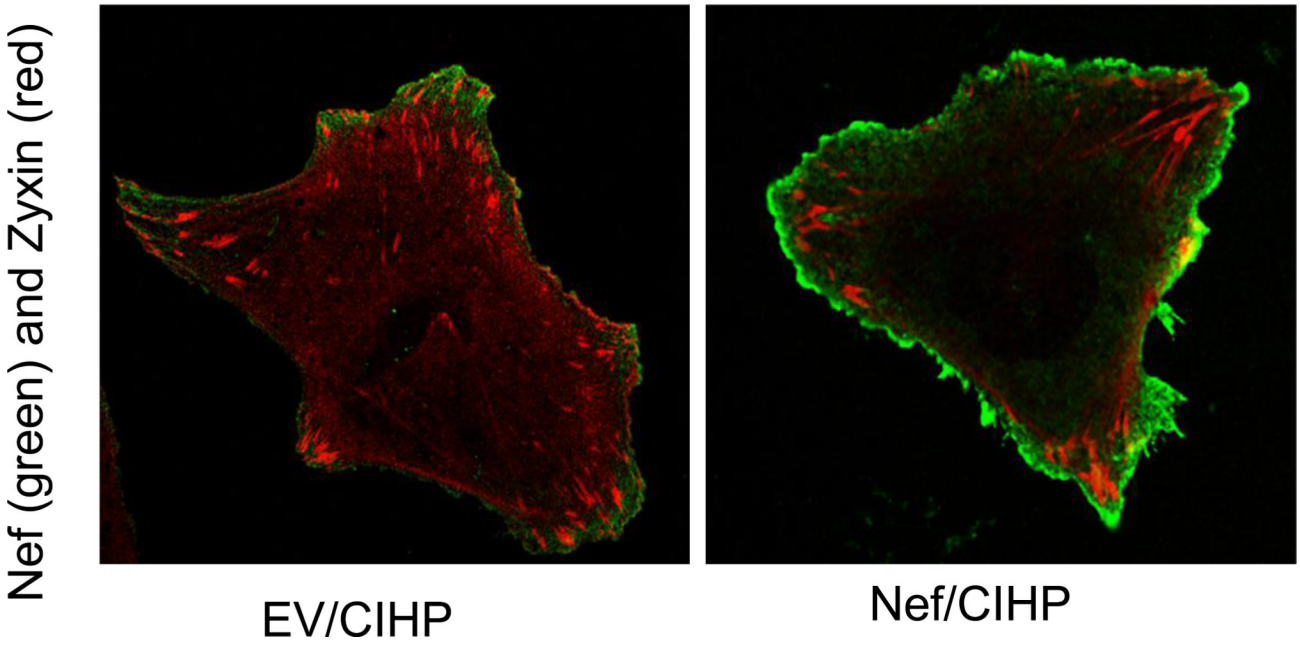

5. Nef/CIHPs display co-localization of Nef with zyxin

EV/CIHPs and Nef/CIHPs weer immunolabeled for Nef and zyxin. Nef/CIHPs showed points of co-localization of Nef and zyxin by displaying orange and yellow fluorescence.

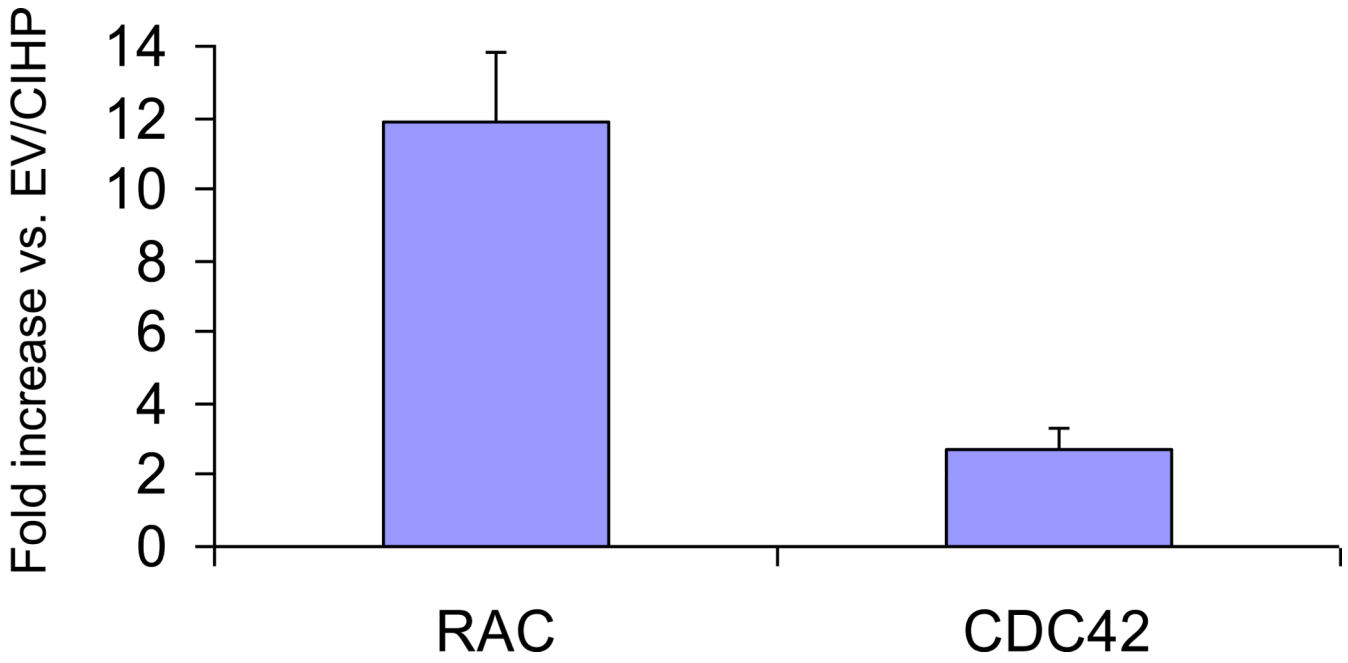

6. Nef/CIHPs showed enhanced expression of Rac1 and CDC42

Total RNAs were extracted from Nef/CIHPs and EV/CIHPs (n=2). Microarray analysis was performed in duplicate samples with an Illumina Human V2-bead chip for 45,000 genes. In Nef/CIHPs, a total of 5,000 genes showed either upregulation or downregulation compared with vector-expressing podocytes. Nef/CIHPs showed several fold upregulation of RAC and CDC42 when compared EV/CIHPs.

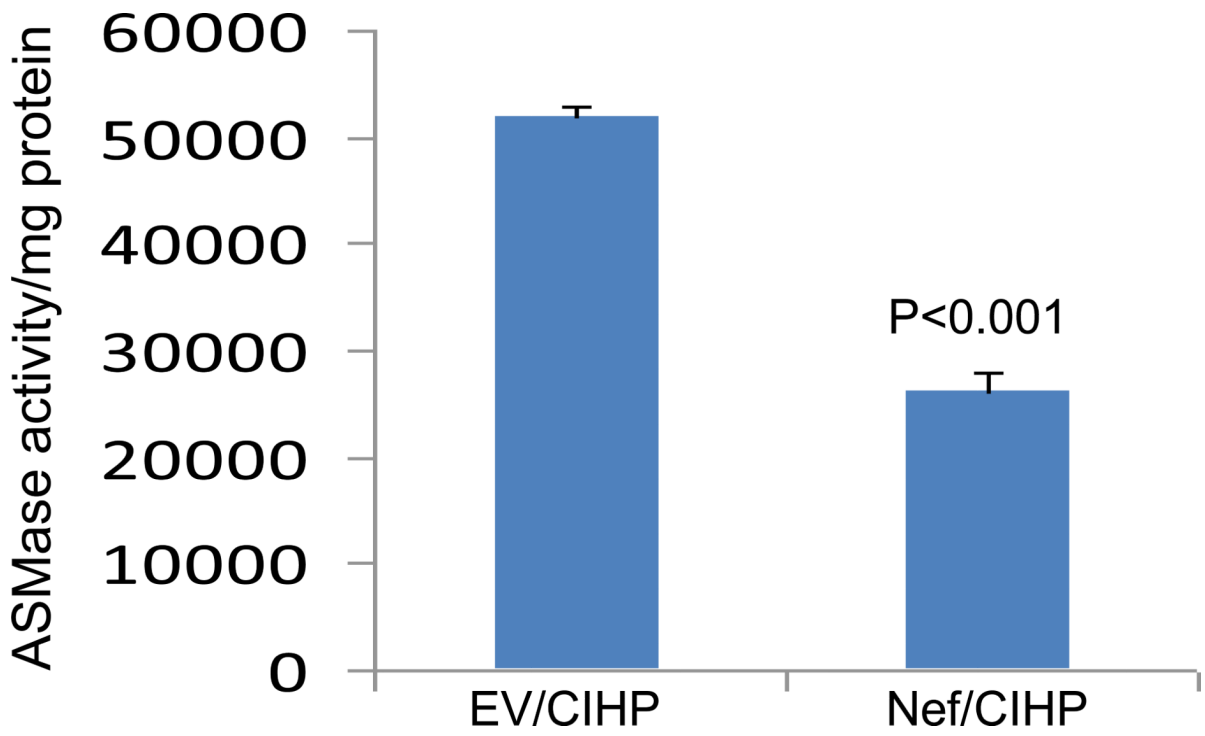

7. Nef/CHPs display attenuated ASMase activity

Cellular lysates of EV/CIHPs and Nef/CIHPs were assayed for ASMase activity. EV/CIHPs displayed attenuated ASMase activity.

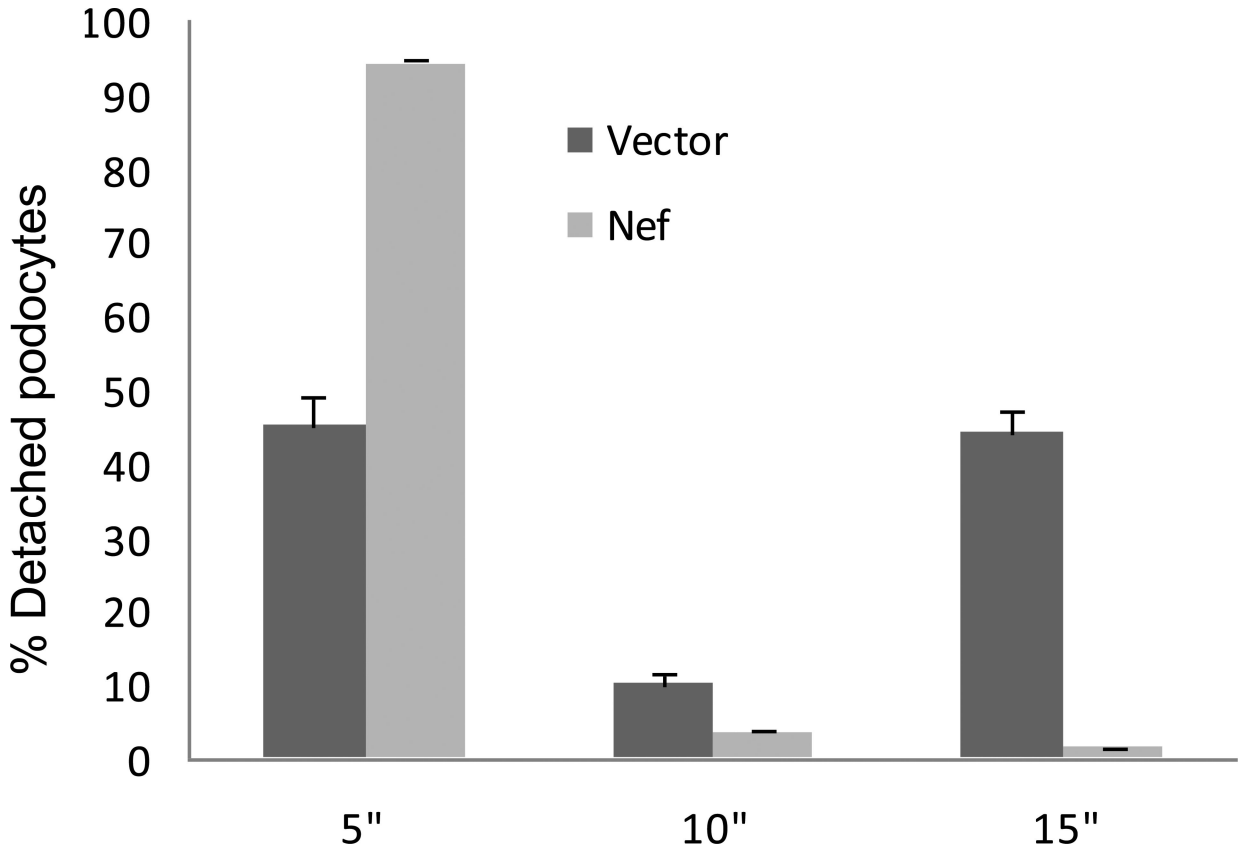

8. Nef enhances podocyte detachment

Deatachment assay was carried on EV/CIHPs and Nef/CIHP grown in Petri dishes. Cells were washed and added 0.5% trypsin and incubated at 37°C for 5, 10 and 15 minutes. Floating cells were counted bya hemocytometer at the indicated time points. Percentage of the detached cells was calculated for each time period. Results are shown as means ± SD form four sets of experiments, each carried out in triplicate.

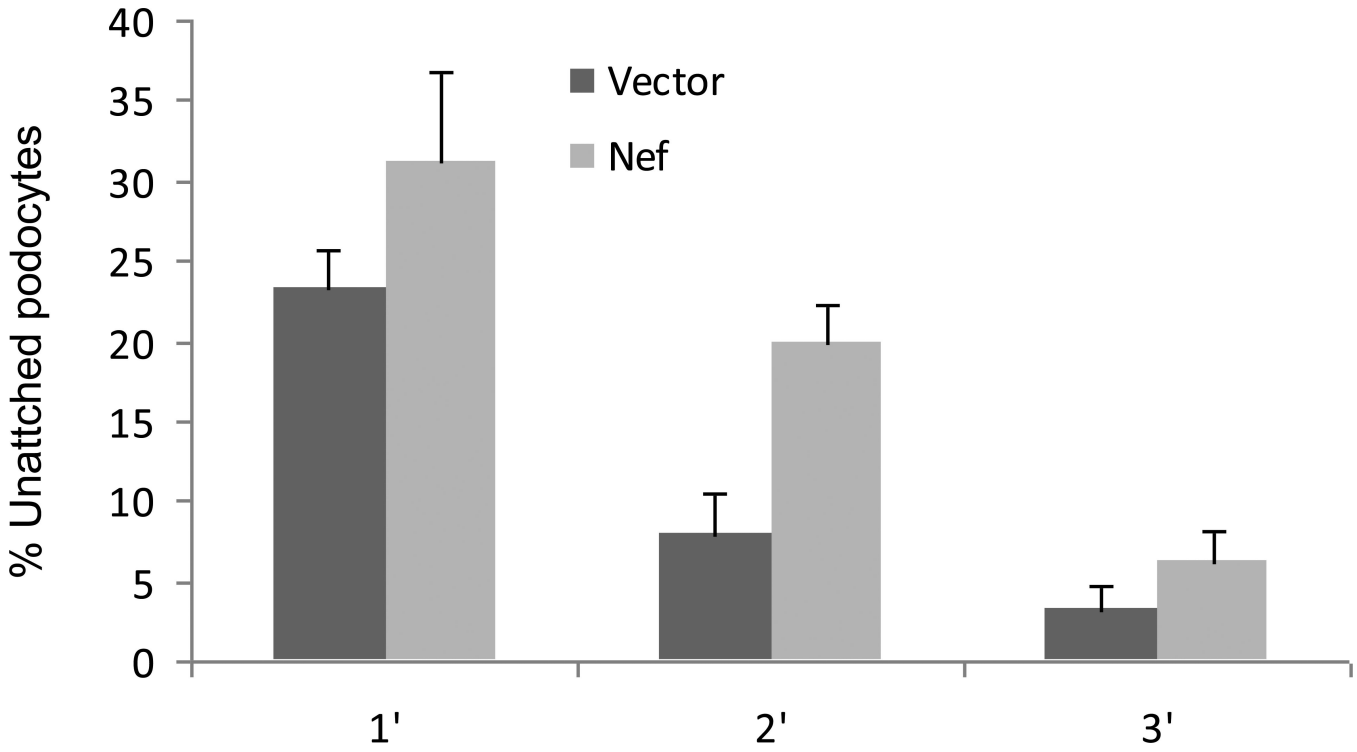

9. Nef decreases podocyte attacment

Equal number of Nef/CHPs and EV/CIHPs were plated into 24-well plates. Numbers of unattached cells in the media, were counted at the indicated time periods. Results are shown as means ± SD from four sets of experiments, each carried out in triplicate.